AIAA JOURNAL
Vol. 43, No. 6, June 2005

Probability of Failure of Composite Cylinders Subjected to Axisymmetric Loading

Hazem E. Soliman* and Rakesh K. Kapania†
Virginia Polytechnic Institute and State University, Blacksburg, Virginia 24061

The effect of uncertainty in applied loads, helix angles, and failure stresses on the probability of failure of composite cylinders was studied. Also, the effect of the factor of safety on the probability of failure of the cylinder was studied. The probability of failure for a composite cylinder subject to axisymmetric loading was obtained using the first-order reliability method (FORM). The failure of the cylinder was studied based on first ply failure. Ply failure was predicted using the non-smooth Hashin criterion. The Hashin criterion is based on writing a different interaction equation for separate failure modes. Four failure modes are considered associated with matrix or fiber failure in either tension or compression. The accuracy of FORM as applied to this problem was verified by comparing the FORM results with those obtained by a Monte Carlo simulation method with importance sampling.

Nomenclature

F	=	applied axial force
g	=	limit state function
k, r	=	layer indices
m	=	number of applied loads
N	=	number of layers
n	=	number of variables
p	=	applied internal pressure
T	=	applied torque
X_i	=	reduced design parameters
x_i	=	design parameters
α	=	layer helix angle
β	=	failure index
μ_{x_i}	=	mean values of design parameters
σ_A^+	=	tensile failure stress in fiber direction
σ_A^-	=	compressive failure stress in fiber direction (absolute value)
σ_T^+	=	tensile failure stress transverse to fiber direction
σ_T^-	=	compressive failure stress transverse to fiber direction (absolute value)
σ_{x_x}	=	standard deviation of design parameters
σ_1	=	stress in fiber direction in material principal coordinate system
σ_2	=	stress in fiber in transverse direction in material principal coordinate system
τ_A	=	failure shear stress in fiber direction
τ_T	=	transverse failure shear stress
τ_{12}	=	shear stress in plane 1–2 in material principal coordinate system

Introduction

COMPOSITE cylinders are used in many important applications. Aircraft fuselages, gas and liquid tanks, and gun barrels are just a few examples. The prediction of the stress field in anisotropic cylinders is, thus, of great practical importance. The stress field in thick composite cylinders is far from uniform, especially if the diameter to thickness ratio is low. On the other hand, thin cylinders lend themselves to shell-type analysis.

Composite circular cylinders were studied extensively in the late 1960s and early 1970s. Pagano[1] developed a general elasticity solution for an anisotropic cylinder under two-dimensional surface tractions that are independent of the axial coordinate. Pagano and Whitney[2] developed a procedure to determine the geometry of a multilayer composite cylinder under specified load conditions by combining a modified plane strain elasticity solution with shell theory. From Pagano's and Pagano and Whitney's work, one can safely conclude that the predictions of classical lamination theory are accurate for thin cylinders away from the cylinder edges. McMurray and Hyer[3] studied the failure characteristics of the elliptical composite cylinders, comparing the response of the elliptical cylinders to the response of the circular cylinder to illustrate the influence of the elliptical geometry on the response of the composite cylinder to an internal pressure. Sherrer[4] presented a theoretical elastic solution for filament wound cylinders with any number of layers. The cylinder is subject to axial, torsion, or pressure loads. Tutuncu and Winckler[5] studied the stresses and deformations in composite cylindrical tubes as a result of combined axisymmetric loading and temperature gradient through the wall thickness using a displacement-based linear elasticity solution to predict the stresses in the thickness direction for thick-walled tubes.

Yang et al.[6] developed an analytical model for the buckling of an orthotropic composite pipe subject to an external pressure. They used the first-order laminated anisotropic plate theory to construct the models of the kinematics and constitutive behavior of the pipe and then used the Ritz method to determine the buckling load under external pressure. Hwang et al.[7] predicted the probabilistic deformation and strength of composite cylinders subject to internal pressure analytically and experimentally. In the analytical solution, they considered uncertainty in three random variables (elastic constants, lamina strengths, and layer thickness). Na and Librescu[8] studied the dynamic response of anisotropic cantilevered thin-walled beams subject to blast and sonic boom loading. Lin and Kam[9] conducted a probabilistic failure analysis for composite plates using stochastic finite element analysis with system parameters taken to be material properties, plate thickness, and lamina strengths.

The goal of the proposed work is to study the effects of uncertainty in helix angles and/or in the applied loads and/or in the values of the failure stresses on the failure of multilayered composite circular cylinders under combined axisymmetric loads (internal pressure, axial force, and torsion). The stress field in a multilayered composite cylinder is obtained by using the shell theory. For axisymmetric loads, the shell theory solution is particularly simple and is computationally inexpensive. Failure analysis is carried out

Received 13 April 2004; presented as Paper 2004-4342 at the AIAA/ISSMO 10th Multidisciplinary Analysis and Optimization Conference, Albany, NY, 30 August–1 September 2004; revision received 20 December 2004; accepted for publication 7 January 2005.

*Graduate Research Assistant, Department of Aerospace and Ocean Engineering; hsoliman@vt.edu. Student Member AIAA.

†Professor, Department of Aerospace and Ocean Engineering; rkapania@vt.edu. Associate Fellow AIAA.

by assuming a first-ply failure. Ply failure is predicted using the Hashin failure criterion.[10] Four failure modes are identified, and a different stress interaction equation is proposed for each one of the different modes, thus producing a piecewise smooth failure surface. Thus, the determination of the probability of failure will involve a piecewise smooth limit state.

The probability of failure is first obtained by using the Monte Carlo simulation method with importance sampling.[11] The importance sampling technique[11] used is the one in which the center of the normal distribution is transformed to the most probable failure point. These results are used as a benchmark to validate the results obtained from a more economical method. Because for a general geometry and loading the use of Monte Carlo simulation, even with importance sampling, is prohibitively expensive, it is natural to seek alternatives that are both simpler and computationally inexpensive. The first-order reliability method (FORM) also known as the Hasofer–Lind method (see Ref. 12), in the authors' views, satisfies this requirement. Nevertheless, it involves certain assumptions about the nature of the limit state. From that perspective, a validation of the FORM as applied to the Hashin criterion is an important task. A comparison is made between the Monte Carlo simulation performed with importance sampling method and the FORM method. The FORM results show very good agreement with simulation results for the case considered. We then address the conditions under which the inclusion of uncertainty in helix angle(s) and failure stresses become important. This work will also explore the effect of using safety factors on the probability of failure in composite design.

Stresses

The stress field in the cylinder is obtained by using the classical lamination theory.[13] For a cylinder under a combination of axisymmetric loads (axial force F, internal pressure p, and torque T), the values of the resultant stresses and moments are obtained in the global cylindrical coordinate system x–θ–r, as follows:

$$N_x = F/2\pi R_0, \qquad N_\theta = pR_0, \qquad N_{x\theta} = T\big/2\pi R_0^2 \tag{1a}$$

$$M_x = 0, \qquad M_\theta = 0, \qquad M_{x\theta} = 0 \tag{1b}$$

where R_0 is the mean radius of the cylinder.

The relation that relates the resultant stresses and moments to the strains and curvatures at the reference surface[13] is represented by

$$\begin{Bmatrix} N \\ M \end{Bmatrix} = \begin{bmatrix} A & B \\ B & D \end{bmatrix} \begin{Bmatrix} \varepsilon^0 \\ \kappa^0 \end{Bmatrix} \tag{2}$$

where A, B, and D are the lamination matrices whose components are given as[13]

$$A_{ij} = \sum_{k=1}^{N} \bar{Q}_{ij}^k (z^k - z^{k-1})$$

$$B_{ij} = \frac{1}{2} \sum_{k=1}^{N} \bar{Q}_{ij}^k [(z^k)^2 - (z^{k-1})^2]$$

$$D_{ij} = \frac{1}{3} \sum_{k=1}^{N} \bar{Q}_{ij}^k [(z^k)^3 - (z^{k-1})^3] \tag{3}$$

where N is the number of layers, k is the layer index, z is the distance through the thickness measured from the reference surface, and $\bar{Q}_{ij}^k$ is the stiffness matrix for the layer k.

We can then obtain the strains and curvatures at the reference surface by substituting the resultant stresses and moments obtained from Eqs. (1) into Eq. (2).

The strain distribution through the thickness is then obtained by using the Kirchhoff hypotheses (see Ref. 13), namely,

$$\{\varepsilon'\} = \{\varepsilon^0 + z\,\kappa^0\} \tag{4}$$

where

$$\{\varepsilon'\} = \begin{Bmatrix} \varepsilon_x \\ \varepsilon_\theta \\ \varepsilon_{x\theta} \end{Bmatrix} \tag{5}$$

The strain vector ε' is then transformed through a strain transformation equation[13] to obtain the strains in the principal material coordinate system. We then substitute the strains obtained in the principal material coordinate system into a stress strain relation to obtain the stress distribution through the thickness in the material principal coordinate system.

Hashin Failure Criterion

The Hashin failure criterion[10] consists of two primary failure modes: a fiber mode in which the composite fails due to fiber rupture in tension or because of fiber buckling in compression, and a matrix mode in which a plane crack parallel to the fibers occurs. Each of the two primary failure modes consists of two cases of failure, a tensile failure mode and a compressive failure mode. That gives us a total of four different failure modes. The equations governing the failure for each of the four modes are as follows:

For the fiber tensile mode ($\sigma_1 > 0$),

$$\left(\sigma_1\big/\sigma_A^+\right)^2 + (\tau_{12}/\tau_A)^2 < 1 \tag{6}$$

where σ_A^+ is the tensile failure stress in the fiber direction, τ_A is the failure shear stress in the fiber direction, and σ_1 is the stress in the fiber direction in the material principal coordinate system.

For the fiber compressive mode ($\sigma_1 < 0$),

$$-\sigma_1\big/\sigma_A^- < 1 \tag{7}$$

where σ_A^- is the compressive failure stress in the fiber direction (absolute value).

For the matrix tensile mode ($\sigma_2 > 0$),

$$\left(\sigma_2\big/\sigma_T^+\right)^2 + (\tau_{12}/\tau_A)^2 < 1 \tag{8}$$

where σ_T^+ is the tensile failure stress transverse to the fiber direction, τ_{12} is the shear stress in the plane 1–2 in the material principal coordinate system, and σ_2 is the stress in the fiber in the transverse direction in the material principal coordinate system.

For the matrix compressive mode ($\sigma_2 < 0$),

$$\left(\sigma_2\big/\sigma_T^-\right)\left[\left(\sigma_T^-\big/2\tau_T\right)^2 - 1\right] + (\sigma_2/2\tau_T)^2 + (\tau_{12}/\tau_A)^2 < 1 \tag{9}$$

where σ_T^- is the compressive failure stress transverse to the fiber direction (absolute value) and τ_T is the transverse failure shear stress.

FORM (Hasofer–Lind Method)

First, we define the failure surface (limit state) as the boundary between the safe and unsafe regions in the design parameter space. The limit state also represents the state beyond which the structure can no longer fulfill the function for which it was designed. The mathematical definition of the limit state is

$$g(x_1, x_2, \ldots, x_n) = 0 \tag{10}$$

where x_i are the random variables (design parameters) of the problem, $g(x_i)$ is the functional relationship among the variables of the problem, and n is the number of variables.

The FORM defines the variables in a reduced form as

$$X_i = \left(x_i - \mu_{x_i}\right)\big/\sigma_{x_i} \tag{11}$$

where μ_{x_i} are the mean values of the random variables, σ_{x_i} are the standard deviations of the random variables, and X_i is a random variable with zero mean and unit standard deviation (reduced form).

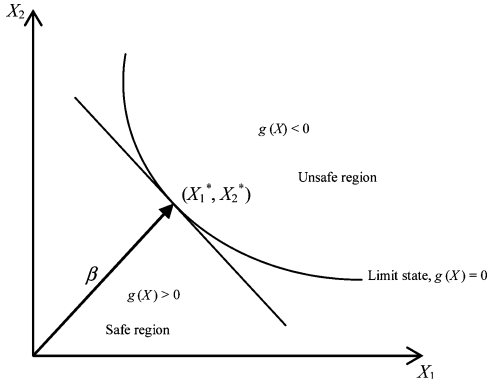

Fig. 1 Limit state of problem with two variables in reduced coordinate system.

With the use of Eq. (11), the limit state (failure surface) $g(x) = 0$ is transformed to the reduced limit state $g(X) = 0$. The x-coordinate system is referred to as the original coordinate system. The X-coordinate system is referred to as the transformed or reduced coordinate system. The origin of the reduced coordinate system is the mean values of the original random variables x_i. Figure 1 shows the limit state for a problem with two design parameters X_1 and X_2 in the reduced coordinate system.

Another important definition to be represented is the definition of the safety index β. The safety index is defined as the minimum distance from the origin of the axes in the reduced coordinate system to the limit state surface (Fig. 1). The point (X_1^*, X_2^*) is then defined as the most probable failure point. The failure index is expressed as

$$\beta = \sqrt{(\boldsymbol{X}^*)^t(\boldsymbol{X}^*)} \tag{12}$$

In our problem, the variables are assumed to have normal distribution. First, we define the function D as the square of the distance from the origin of the axes in the reduced coordinate system to any point on the limit state:

$$D = \sum_{i=1}^{n} \left(\frac{x_i - \mu_{x_i}}{\sigma_{x_i}} \right)^2 \tag{13}$$

The safety index β is then

$$\beta = \sqrt{D_{\min}} \tag{14}$$

Define the load vector $\boldsymbol{F} = \{f_1 \;\; f_2 \;\; f_3 \;\; \ldots \;\; f_m\}^t$, and the helix angle vector as $\boldsymbol{\acute{a}} = \{\alpha_1 \;\; \alpha_2 \;\; \alpha_3 \;\; \ldots \;\; \alpha_N\}$. The stresses then are obtained as a linear combination the stresses resulting from applying unit loads separately:

$$\sigma_{jk}(\boldsymbol{\acute{a}}, \boldsymbol{F}) = \sum_{i=1}^{m} \sigma_{jk}^{(i)} f_i \tag{15}$$

where σ_{jk} are the stress components and $\sigma_{jk}^{(i)}$ are the stress components resulting from applying a unit load f_i.

The limit state is then obtained by substituting with the stresses obtained from Eq. (15) into the Hashin failure criterion equations (6–9). The failure index is obtained by finding the minimum of the function D [Eq. (13)] for each of the failure modes. When solving the optimization problem for D, we normalize each of the stress components in the constraints by their respective failure stress values. The following are the failure modes considered in this study.

For the fiber tensile mode ($\sigma_1 > 0$), minimize

$$D = \sum_{i=1}^{n} \left(\frac{x_i - \mu_{x_i}}{\sigma_{x_i}} \right)^2$$

subject to the constraints

$$\sum_{i=1}^{n} \frac{\sigma_1^i}{\sigma_A^+} f_i \geq 0 \tag{16a}$$

$$\sum_{i=1}^{m}\sum_{j=1}^{m} \left[\left(\frac{\sigma_1^i}{\sigma_A^+} \right)\left(\frac{\sigma_1^j}{\sigma_A^+} \right) + \left(\frac{\tau_{12}^i}{\tau_A} \right)\left(\frac{\tau_{12}^j}{\tau_A} \right) \right] f_i f_j = 1 \tag{16b}$$

For the fiber compressive mode ($\sigma_1 < 0$), minimize

$$D = \sum_{i=1}^{n} \left(\frac{x_i - \mu_{x_i}}{\sigma_{x_i}} \right)^2$$

subject to the constraints

$$\sum_{i=1}^{n} \frac{\sigma_1^i}{\sigma_A^-} f_i \leq 0 \tag{17a}$$

$$\sum_{i=1}^{m} -\left(\frac{\sigma_1^i}{\sigma_A^-} \right) f_i = 1 \tag{17b}$$

For the matrix tensile mode ($\sigma_2 > 0$), minimize

$$D = \sum_{i=1}^{n} \left(\frac{x_i - \mu_{x_i}}{\sigma_{x_i}} \right)^2$$

subject to the constraints

$$\sum_{i=1}^{m} \frac{\sigma_2^i}{\sigma_T^+} f_i \geq 0 \tag{18a}$$

$$\sum_{i=1}^{m}\sum_{j=1}^{m} \left[\left(\frac{\sigma_2^i}{\sigma_T^+} \right)\left(\frac{\sigma_2^j}{\sigma_T^+} \right) + \left(\frac{\tau_{12}^i}{\tau_A} \right)\left(\frac{\tau_{12}^j}{\tau_A} \right) \right] f_i f_j = 1 \tag{18b}$$

For the matrix compressive mode, minimize

$$D = \sum_{i=1}^{n} \left(\frac{x_i - \mu_{x_i}}{\sigma_{x_i}} \right)^2$$

subject to the constraints

$$\sum_{i=1}^{m} \frac{\sigma_2^i}{\sigma_T^-} f_i \leq 0 \tag{19a}$$

$$\left[\left(\frac{\sigma_T^-}{2\tau_t} \right)^2 - 1 \right] \sum_{i=1}^{m} \left(\frac{\sigma_2^i}{\sigma_T^-} \right) f_i + \sum_{i=1}^{m}\sum_{j=1}^{m} \left[\left(\frac{\sigma_2^i}{2\tau_T} \right)\left(\frac{\sigma_2^j}{2\tau_T} \right) + \left(\frac{\tau_{12}^i}{\tau_A} \right)\left(\frac{\tau_{12}^j}{\tau_A} \right) \right] f_i f_j = 1 \tag{19b}$$

Sensitivity

To account for the effect of uncertainty in the applied loads, helix angles, and failure stresses, sensitivities of the failure equation of each of the failure modes to these parameters has to be obtained.

Applied Loads

In the four modes of failure, the stresses σ_1, σ_2, and τ_{12} are the only dependents on the applied loads. To calculate the sensitivity of the stresses to the applied loads, we first obtain the derivatives of the stress and moment resultants with respect to the applied loads vector $\boldsymbol{F}$. This is obtained by differentiating Eqs. (1) with respect to the applied loads. From Eqs. (1), the derivatives of N_x with respect to the internal pressure and torque are identically zero. Also, the derivatives of N_θ with respect to the axial force and the applied torque, and the derivatives of $N_{x\theta}$ with respect to the axial force and

the internal pressure, are all identically zero. Also, the derivatives of all of the bending and twisting moment resultants with respect to all of the applied loads are zero because the bending and twisting moment resultants are zero in the case of axisymmetric loading. The only derivatives obtained from differentiating Eqs. (1) with respect to the load vector are

$$\frac{\partial N_x}{\partial F} = \frac{1}{2\pi R_0}, \qquad \frac{\partial N_\theta}{\partial p} = R_0, \qquad \frac{\partial N_{x\theta}}{\partial T} = \frac{1}{2\pi R_0^2} \tag{20}$$

Differentiating Eq. (2) with respect to the applied loads vector

$$\begin{Bmatrix} \varepsilon^0 \\ \kappa^0 \end{Bmatrix}_{,F} = \begin{bmatrix} A & B \\ B & D \end{bmatrix}^{-1} \begin{Bmatrix} N \\ M \end{Bmatrix}_{,F} \tag{21}$$

we then obtain the derivatives of the strains and curvatures at the mean radius of the cylinder by substituting Eq. (20) into Eq. (21). Differentiating Eq. (4) with respect to the applied loads vector, we get

$$\{\varepsilon'\}_{,F} = \{\varepsilon^0 + z\kappa^0\}_{,F} \tag{22}$$

On substitution of the derivatives of the strains and curvatures at the mean radius of the cylinder obtained from Eq. (21) into Eq. (22), we then have the derivatives of the strains in the global cylindrical coordinate system with respect to the applied loads vector. We then obtain the derivatives of the strains in the material principal coordinate system by substituting Eq. (22) into Eq. (23), which represents the derivative of the transformation equation[13] that transforms the strains from the global coordinate system to the material principal coordinate system with respect to the applied loads vector

$$\{\varepsilon\}_{,F} = [T]\{\varepsilon'\}_{,F} \tag{23}$$

The stress strain relation is then differentiated with respect to the load vector, as follows:

$$\{\sigma\}_{,F} = [Q]\{\varepsilon\}_{,F} \tag{24}$$

Substituting the derivatives of the strains in the material principal coordinate system obtained from Eq. (23) into Eq. (24), we then have the derivatives of the stresses with respect to the applied loads.

Helix Angles

The case of calculating the sensitivity for the helix angles is similar to that for the applied loads because only the stresses σ_1, σ_2, and τ_{12} in all of the equations of the failure modes are the only dependents on the helix angles. The only difference is that the helix angle is different for each layer. For this reason, we will use two indices for the layers, k and r. The index k will be used to denote the layer at which we are calculating the sensitivity, and the index r will be used to denote the layer that we are differentiating with respect to its helix angle. For example, $\{\sigma\}^k_{,\alpha_r}$ represents the derivative of the stresses in the layer k with respect to the helix angle of the layer r.

First, we will obtain the derivatives of the lamination matrices A, B, and D [Eqs. (3)] of the layer k with respect to the helix of the layer r. Because $\bar{Q}^k$ is a function of α_k only, the derivatives of the lamination matrices will be

$$A_{ij,\alpha_r} = \sum_{k=1}^{N} \delta_{rk} \bar{Q}^k_{ij,\alpha_k} (z^k - z^{k-1})$$

$$B_{ij,\alpha_r} = \frac{1}{2} \sum_{k=1}^{N} \delta_{rk} \bar{Q}^k_{ij,\alpha_k} [(z^k)^2 - (z^{k-1})^2]$$

$$D_{ij,\alpha_r} = \frac{1}{3} \sum_{k=1}^{N} \delta_{rk} \bar{Q}^k_{ij,\alpha_k} [(z^k)^3 - (z^{k-1})^3] \tag{25}$$

Next, we differentiate Eq. (2) to obtain the derivative of the strains and curvatures at the mean radius of the cylinder by the use of the resulting derivatives of Eq. (25) with respect to the helix angle of the layer r:

$$\begin{Bmatrix} \varepsilon^0 \\ \kappa^0 \end{Bmatrix}_{,\alpha_r} = -\begin{bmatrix} A & B \\ B & D \end{bmatrix}^{-1} \begin{bmatrix} A & B \\ B & D \end{bmatrix}_{,\alpha_r} \begin{Bmatrix} \varepsilon^0 \\ \kappa^0 \end{Bmatrix} \tag{26}$$

The derivatives of the strains through the thickness of the layer k with respect to the helix angle of the layer r in the global cylindrical coordinate system are then obtained by substituting these derivatives (26) into Eq. (27), resulting from differentiating Eq. (4):

$$\{\varepsilon'\}^k_{,\alpha_r} = \{\varepsilon^0\}^k_{,\alpha_r} + z^k \{\kappa^0\}^k_{,\alpha_r} \tag{27}$$

To obtain the derivatives of the strains in the material principal coordinate system for layer k with respect to the helix angle of layer r, we differentiate the strains transformation equation[13] and then use Eq. (27) to substitute for the derivatives of the strains in the global cylindrical coordinate system

$$\{\varepsilon\}^k_{,\alpha_r} = \delta_{rk}[T]^k_{,\alpha_k}\{\varepsilon'\}^k + [T]^k\{\varepsilon'\}^k_{,\alpha_r} \tag{28}$$

Differentiating the stress strain relation equation[13] to obtain an expression for the derivatives of the stresses in layer k with respect to the helix angle of layer r in the material principal coordinate system, we then get

$$\{\sigma\}^k_{,\alpha_r} = [Q]\{\varepsilon\}^k_{,\alpha_r} \tag{29}$$

On substitution of the derivatives of the strains obtained through Eq. (28) into Eq. (29), we then have the sensitivity of the stresses to the helix angles.

Failure Stresses

The sensitivity analysis for the failure stresses is more difficult than the analysis for the applied loads and helix angles. In this sensitivity analysis, the differentiation will be applied directly to the constraints of the optimization problem. First, we define the vector $\boldsymbol{S}$ as follows:

$$\boldsymbol{S} = \begin{Bmatrix} \sigma_A^+ & \sigma_A^- & \sigma_T^+ & \sigma_T^- & \tau_A & \tau_T \end{Bmatrix}^T$$

$$= \{S_1 \quad S_2 \quad S_3 \quad S_4 \quad S_5 \quad S_6\}^T \tag{30}$$

Then we define the normalized vector $\hat{\boldsymbol{S}}$, namely,

$$\hat{\boldsymbol{S}}_j = S_j \big/ \mu_{S_j}, \qquad j = 1, 2, \ldots, 6 \tag{31}$$

The same steps are then followed for each failure mode to obtain the sensitivity information. With regard to the fiber tensile mode, for simplicity, we set the following definitions:

$$a_i = \left(\frac{\sigma_1^i}{\sigma_A^+}\right), \qquad b_i = \left(\frac{\tau_{12}^i}{\tau_A}\right)$$

$$A_{ij} = \left[\left(\frac{\sigma_1^i}{\sigma_A^+}\right)\left(\frac{\sigma_1^j}{\sigma_A^+}\right) + \left(\frac{\tau_{12}^i}{\tau_A}\right)\left(\frac{\tau_{12}^j}{\tau_A}\right)\right]$$

$$\boldsymbol{A} = \boldsymbol{a}\boldsymbol{a}^T + \boldsymbol{b}\boldsymbol{b}^T$$

$$\frac{\partial a_i}{\partial S_j} = 0 \qquad \text{for} \qquad j = 2, 3, 4, 5, 6$$

$$\frac{\partial a_i}{\partial \hat{S}_1} = \frac{\partial a_i}{\partial S_1}\frac{\partial S_1}{\partial \hat{S}_1} = \mu_{S_1}\frac{\partial a_i}{\partial S_1} = \mu_{S_1}\left(\frac{-\sigma_1^i}{S_1^2}\right) = -a_i\frac{\mu_{S_1}}{S_1}$$

$$\frac{\partial a_i}{\partial \hat{S}_i} = -\frac{a_i}{\hat{S}_i} \tag{32a}$$

Similarly,

$$\frac{\partial b_i}{\partial S_j} = 0 \qquad \text{for} \qquad j = 1, 2, 3, 4, 6$$

$$\frac{\partial b_i}{\partial \hat{S}_5} = -\frac{b_i}{\hat{S}_5} \tag{32b}$$

$$\frac{\partial A_{ij}}{\partial \hat{S}_j} = \left[-\left(\frac{a_i}{\hat{S}_1}\right)a_i^T - \left(\frac{b_i}{\hat{S}_5}\right)b_i^T\right] + \left[-a_i\left(\frac{a_i}{\hat{S}_1}\right)^T - b_i\left(\frac{b_i}{\hat{S}_5}\right)^T\right] \tag{32c}$$

For the fiber compressive mode,

$$a_i = \left(\frac{\sigma_1^i}{\sigma_A^-}\right)$$

$$\frac{\partial a_i}{\partial \hat{S}_2} = -\frac{a_i}{\hat{S}_2} \tag{33}$$

For the matrix tensile mode,

$$a_i = \left(\frac{\sigma_2^i}{\sigma_T^+}\right), \qquad b_i = \left(\frac{\tau_{12}^i}{\tau_A}\right)$$

$$A_{ij} = \left[\left(\frac{\sigma_2^i}{\sigma_T^+}\right)\left(\frac{\sigma_2^j}{\sigma_T^+}\right) + \left(\frac{\tau_{12}^i}{\tau_A}\right)\left(\frac{\tau_{12}^j}{\tau_A}\right)\right]$$

$$\boldsymbol{A} = \boldsymbol{a}\boldsymbol{a}^T + \boldsymbol{b}\boldsymbol{b}^T$$

$$\frac{\partial a_i}{\partial \hat{S}_3} = -\frac{a_i}{\hat{S}_3} \tag{34a}$$

$$\frac{\partial b_i}{\partial \hat{S}_5} = -\frac{b_i}{\hat{S}_5} \tag{34b}$$

$$\frac{\partial A_{ij}}{\partial \hat{S}_j} = \left[-\left(\frac{a_i}{\hat{S}_3}\right)a_i^T - \left(\frac{b_i}{\hat{S}_5}\right)b_i^T\right] + \left[-a_i\left(\frac{a_i}{\hat{S}_3}\right)^T - b_i\left(\frac{b_i}{\hat{S}_5}\right)^T\right] \tag{34c}$$

For the matrix compressive mode,

$$a_i = \left(\frac{\sigma_2^i}{2\tau_T}\right), \qquad b_i = \left(\frac{\tau_{12}^i}{\tau_A}\right)$$

$$c_i = \left[\left(\frac{\sigma_T^-}{2\tau_T}\right)^2 - 1\right]\left(\frac{\sigma_2^i}{\sigma_T^-}\right)$$

$$A_{ij} = \left[\left(\frac{\sigma_2^i}{2\tau_T}\right)\left(\frac{\sigma_2^j}{2\tau_T}\right) + \left(\frac{\tau_{12}^i}{\tau_A}\right)\left(\frac{\tau_{12}^j}{\tau_A}\right)\right]$$

$$\boldsymbol{A} = \boldsymbol{a}\boldsymbol{a}^T + \boldsymbol{b}\boldsymbol{b}^T$$

$$\frac{\partial a_i}{\partial \hat{S}_6} = -\frac{a_i}{2\hat{S}_6} \tag{35a}$$

$$\frac{\partial b_i}{\partial \hat{S}_5} = -\frac{b_i}{\hat{S}_5} \tag{35b}$$

$$\frac{\partial A_{ij}}{\partial \hat{S}_j} = \left[-\left(\frac{a_i}{2\hat{S}_6}\right)a_i^T - \left(\frac{b_i}{\hat{S}_5}\right)b_i^T\right] + \left[-a_i\left(\frac{a_i}{2\hat{S}_6}\right)^T - b_i\left(\frac{b_i}{\hat{S}_5}\right)^T\right] \tag{35c}$$

$$\frac{\partial c_i}{\partial \hat{S}_4} = \frac{1}{\hat{S}_4}\left[\left(\frac{S_4}{2S_6}\right)^2 + 1\right]\left(\frac{\sigma_2^i}{S_4}\right) \tag{35d}$$

$$\frac{\partial c_i}{\partial \hat{S}_6} = \frac{1}{\hat{S}_6}\left[-\left(\frac{S_4}{2S_6^2}\right)\sigma_2^i\right] \tag{35e}$$

Results

A four-layered $(\pm 30 \text{ deg})_s$ composite circular cylinder of graphite epoxy was studied. The material and geometric properties of a layer of graphite epoxy are taken to be $E_1 = 155$ GPa, $E_2 = 12.1$ GPa, $\nu_{12} = 0.248$, $G_{12} = 4.4$ GPa, $\sigma_A^+ = 1.482$ GPa, $\sigma_A^- = 1.241$ GPa, $\sigma_T^+ = 50.0$ MPa, $\sigma_T^- = 200.0$ MPa, $\tau_A = 100.0$ MPa, $\tau_T = 100.0$ MPa, $R_0 = 0.4$ m, and $t = 0.008$ m, where t is the thickness of the cylinder.

Four cases were studied. In the first case, the cylinder was studied subject to an internal pressure and axial force. Two cases of uncertainty were considered. First, the uncertainty was considered in the applied loads only, and then it was considered in both the applied loads and the failure stresses. Results for this case were obtained by using both the Monte Carlo simulation with importance sampling[11] and the FORM,[12] and a comparison was made between the two methods.

The second case was meant to study the effect of uncertainty in the failure stresses on the failure of the cylinder. The probability of failure was obtained for the cylinder subject to an internal pressure and an axial force by using the FORM for two cases of uncertainty. In the first case, the uncertainty was considered in the applied loads only, and then it was considered in both the applied loads and the failure stresses. The results will be shown together to show the effect of uncertainty in the failure stresses on the failure of the cylinder (Fig. 2).

In the third case, the effect of uncertainty in the helix angles on the failure of the cylinder when subject to an internal pressure, and an axial force is studied. The probability of failure was obtained for the cylinder using the FORM for two cases of uncertainty. In the first case, the uncertainty was considered in the applied loads only, and then it was considered in both the applied loads and the helix angles. The results were plotted on the same figure to show the effect of uncertainty in the helix angles on the failure of the cylinder (Fig. 3).

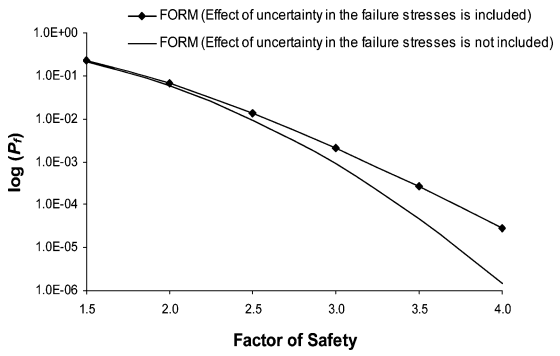

Fig. 2 Effect of uncertainty in failure stresses on the probability of failure.

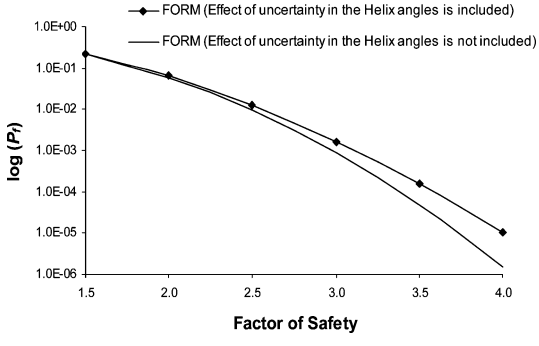

Fig. 3 Effect of uncertainty in helix angles on the probability of failure.

The fourth case studies the effect of the factor of safety on the probability of failure. Three combinations of loading were considered, and the probability of failure was obtained for different values of factor of safety for each combination.

FORM vs Monte Carlo

To obtain the probability of failure considering the uncertainty, results were first obtained using the Monte Carlo simulation with importance sampling[11] applied to the Hashin failure criterion. Results were also obtained by using the FORM.[12] Results from the Monte Carlo simulation with importance sampling were used as a benchmark to validate the accuracy of the FORM. A comparison between the two methods was made, and the FORM proved to be very reliable in calculating the probability of failure.

When the uncertainty in the calculation of the probability of failure is considered by using the Monte Carlo simulation with importance sampling, the probability distribution of the ply angles was assumed to be normal with a standard deviation of $\sigma_\alpha = 3$. The probability distributions of the applied loads and the failure stresses were also assumed to be normal. The coefficient of variation for the pressure was taken to be 0.3, the coefficient of variation for the axial force was taken to be 0.2, and the coefficient of variation for the failure stresses was taken to be 0.2.

First, the probability of failure with both the Monte Carlo simulation method with importance sampling[11] and the FORM for different values of factor of safety was calculated. The results were obtained considering the effect of uncertainty in the applied loads only. The cylinder studied is subject to an internal pressure of 6.895×10^9 Pa and an axial force of 2×10^6 N. Figure 4 shows the results for this case, in which the FORM results show a very good agreement with the Monte Carlo simulation method with importance sampling results. The probability of failure was calculated again using both the Monte Carlo simulation method with importance sampling and the FORM for different values of factor of safety considering the effect of uncertainty in both the applied loads and the failure stresses. Figure 5 shows the results for this problem. The FORM results still show a very good agreement with the Monte Carlo simulation method with importance sampling results.

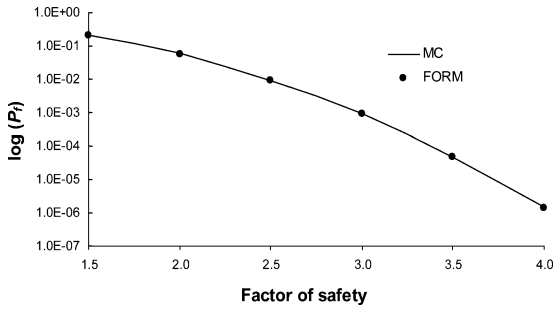

Fig. 4 Monte Carlo with importance sampling vs FORM considering uncertainty in applied loads.

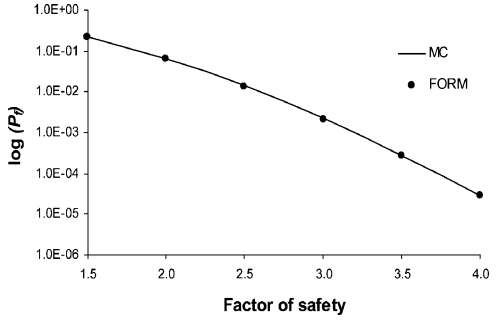

Fig. 5 Monte Carlo with importance sampling vs FORM considering uncertainty in applied loads and failure stresses.

Table 1 Probability of failure for cylinder subject to three different combinations of loading for different values of factor of safety

Factor of safety	Probability of failure		
	$p = 6.895 \times 10^8$ Pa, $F = 1.0 \times 10^6$ N	$p = 1.724 \times 10^9$ Pa, $F = 1.25 \times 10^6$ N	$p = 3.447 \times 10^9$ Pa, $F = 1.5 \times 10^6$ N
1.5	4.0112×10^{-2}	8.8041×10^{-2}	3.2911×10^{-1}
2.0	6.1620×10^{-4}	5.2932×10^{-3}	1.9715×10^{-1}
2.5	4.8904×10^{-6}	1.5554×10^{-4}	1.0641×10^{-1}
3.0	4.4530×10^{-8}	3.4066×10^{-6}	5.1722×10^{-2}
3.5	6.7696×10^{-10}	7.7825×10^{-8}	2.2731×10^{-2}
4.0	5.1868×10^{-10}	2.2746×10^{-9}	9.0959×10^{-3}

Effect of Uncertainty in Failure Stresses on Failure of Cylinder

To study the effect of the uncertainty in the failure stresses, the probability of failure is obtained by using the FORM for different values of factor of safety for two cases. First, the effect of uncertainty is considered only in the applied loads. Second, the effect of uncertainty is considered in both the applied loads and failure stresses. The cylinder studied is subject to an internal pressure of 6.895×10^9 Pa and an axial force of 2×10^6 N.

This study is important because it shows the large role played by the uncertainty in the failure stresses on the failure of the composite cylinder. Figure 2 shows a comparison between the two cases. The effect of the uncertainty in the failure stresses on the failure of the cylinder is obvious at high values of factor of safety where the applied loads have a minor effect on the failure of the cylinder.

Effect of Uncertainty in Helix Angles on Failure of Cylinder

To study the effect of the uncertainty in the helix angles, the probability of failure is obtained by using the FORM for different values of factor of safety for two cases. The first case is that in which the effect of uncertainty is considered only in the applied loads. The second case is that in which the effect of uncertainty is considered in both the applied loads and the helix angles. The cylinder studied is subject to an internal pressure of 6.895×10^9 Pa and an axial force of 2×10^6 N. Figure 3 shows a comparison between the two cases. The effect of the uncertainty in the helix angles on the failure of the cylinder is obvious at high values of factor of safety, the region where the applied loads have a minor effect on the failure of the cylinder.

Effect of Factor of Safety on Probability of Failure

To study the correlation between the factor of safety and the probability of failure, three different combinations of loading were studied, and the probability of failure was obtained for each combination for different values of factor of safety. The cylinder is subject to an internal pressure and an axial force. The values for the load combinations are as follows: $p = 6.895 \times 10^8$ Pa and $F = 1.0 \times 10^6$ N, $p = 1.724 \times 10^9$ Pa and $F = 1.25 \times 10^6$ N, and $p = 3.447 \times 10^9$ Pa and $F = 1.50 \times 10^6$ N.

Table 1 shows the results for the three combinations of loading for different values of factor of safety. Results listed in Table 1 show that although the probability of failure decreases as the factor of safety increases, the correlation between the two is only qualitative.

Conclusions

The determination of the probability of failure of a composite cylinder subject to axisymmetric loading, including uncertainty in applied loads, helix angles, and failure stresses, was considered. First, results were obtained by using the Monte Carlo simulation method with importance sampling. These results were used to validate the adequacy of the FORM method. The effect of uncertainty in helix angles and failure stresses on the probability of failure of the cylinder was studied. The effect of factor of safety on the probability of failure of the cylinder was also studied.

Comparison of the results of the FORM and Monte Carlo simulation method with importance sampling indicates that the FORM is quite reliable in calculating the probability of failure when considering uncertainty in applied loads, helix angles, and failure stresses

for the problem considered. In addition, it is computationally inexpensive compared to the Monte Carlo simulation method with importance sampling.

From the study of the effect of uncertainty in the failure stresses and the helix angles, the uncertainty in the failure stresses and the helix angles were found to play a big role in the determination of the probability of failure of the composite cylinder, especially when designing for a high factor of safety.

Although, as expected, the probability of failure decreases as the factor of safety increases, the correlation between the two is only qualitative. For the same factor of safety, but different nominal loading, the probability of failure can be widely different. This indicates that using static factors of safety in the design procedure of filament wound cylinders is a dubious procedure.

References

[1]Pagano, N. J., "The Stress Field in a Cylindrically Anisotropic Body Under Two-Dimensional Surface Tractions," *Journal of Applied Mechanics,* Vol. 39, Sept. 1972, pp. 791–796.

[2]Pagano, N. J., and Whitney, J. M., "Geometric Design of Composite Cylindrical Characterization Specimens," *Journal of Composite Materials,* Vol. 4, July 1970, pp. 360–378.

[3]McMurray, J. M., and Hyer, M. W., "Response and Failure Characteristics of Internally Pressurized Elliptical Composite Cylinders," *AIAA Journal*, Vol. 40, No. 1, 2002, pp. 117–125.

[4]Sherrer, R. E., "Filament Wound Cylinders with Axi-Symmetric Loads," *Journal of Composite Materials*, Vol. 1, No. 4, 1967, pp. 344–355.

[5]Tutuncu, N., and Winckler, S. J., "Stresses and Deformations in Thick Walled Cylinders Subjected to Combined Loading and a Temperature Gradient," *Journal of Reinforced Plastics and Composites*, Vol. 12, No. 2, 1993, pp. 198–209.

[6]Yang, C., Pang, S., and Zhao, Y., "Buckling Analysis of Thick-Walled Composite Pipe Under External Pressure, *Journal of Composite Materials*, Vol. 31, No. 4, 1997, pp. 409–426.

[7]Hwang, T., Hong, C., and Kim, C., "Probabilistic Deformation and Strength Prediction for a Filament Wound Pressure Vessel," *Composites Engineering, Part B*, Vol. 34, No. 5, 2003, pp. 481–497.

[8]Na, S., and Librescu, L., "Dynamic Response of Cantilevered Thin-Walled Beams to Blast and Sonic-Boom Loadings," *Journal of Shock and Vibration*, Vol. 5, Dec. 1998, pp. 23–33.

[9]Lin, S. C., and Kam, T. Y., "Probabilistic Failure Analysis of Transversely Loaded Laminated Composite Plates Using First-Order Second Moment Method," *Journal of Engineering Mechanics*, Vol. 126, No. 8, 2000, pp. 812–820.

[10]Hashin, Z., "Failure Criteria for Unidirectional Fiber Composites," *Journal of Applied Mechanics*, Vol. 47, No. 2, 1980, pp. 329–334.

[11]Melchers, R. E., *Structural Reliability Analysis and Prediction*, 2nd ed., Wiley, 1999.

[12]Haldar, A., and Mahadevan, S., *Reliability Assessment Using Stochastic Finite Element Analysis*, Wiley, New York, 2000.

[13]Hyer, M. W., and White, S. R., *Stress Analysis of Fiber-Reinforced Composite Materials*, McGraw–Hill, New York, 1997.

B. Sankar
Associate Editor